

AC loss and contact resistance in REBCO CORC[®], Roebel, and stacked tape cables

K Yagotintsev¹, V A Anvar^{1,2,6} , P Gao¹, M J Dhalle¹, T J Haugan³, D C Van Der Laan⁴ , J D Weiss⁴ , M S A Hossain^{2,5}  and A Nijhuis¹ 

¹ University of Twente, Faculty of Science & Technology, 7522 NB Enschede, The Netherlands

² University of Wollongong, Institute for Superconducting and Electronic Materials, Wollongong, Australia

³ US Air Force Research Laboratory, United States of America

⁴ Advanced Conductor Technologies LLC and University of Colorado, Boulder, United States of America

⁵ University of Queensland, School of Mechanical and Mining Engineering, Brisbane QLD 4072, Australia

E-mail: v.a.anvar@utwente.nl

Received 20 February 2020, revised 3 May 2020

Accepted for publication 29 May 2020

Published 2 July 2020



Abstract

Many high-temperature superconductor (HTS) applications require superconducting cables with high currents while operating in an alternating magnetic field. HTS cables should be composed of numerous superconducting tapes to achieve the required current capacity. Alternating current and magnetic fields cause AC losses in such cables and can provoke conductor instability. AC losses and contact resistances were measured of several cable designs based on commercially available REBCO tapes at the University of Twente. The AC loss was measured under identical conditions for eight REBCO conductors manufactured according to three types of cabling methods—CORC[®] (Conductor on Round Core), Roebel, and stacked tape, including a full-size REBCO CICC (cable in conduit conductor). The measurements were done at $T = 4.2$ K without transport current in a sinusoidal AC magnetic field of 0.4 T amplitude and frequencies from 5 to 55 mHz. The AC loss was measured simultaneously by calibrated gas flow calorimeter utilizing the helium boil-off method and by the magnetization method using pick-up coils. Also, the AC loss of two CORC[®] conductors and a Roebel cable was measured at 77 K. Each conductor was measured with and without background field of 1 T. The measured AC coupling loss in the CORC[®] and Roebel conductors is negligible at 4.2 K for the applied conditions while at 77 K coupling loss was observed for all conductors. The absence of coupling loss at 4.2 K can be explained by shielding of the conductor interior; this is confirmed with measurement and calculation of the penetration field of CORC[®] and Roebel cables. The inter-tape contact resistance was measured for CORC[®] and stacked tape samples at 4.2 and 77 K. It was demonstrated that a short heat treatment of CORC[®] conductor with solder-coated tapes activates tape-to-tape soldering and decreases the contact resistance. The reduction of contact resistance by two orders in magnitude to tens of nΩm is comparable with the interstrand contact resistance in ITER Nb₃Sn type conductors.

⁶ Author to whom any correspondence should be addressed.



Original content from this work may be used under the terms of the [Creative Commons Attribution 4.0 licence](https://creativecommons.org/licenses/by/4.0/). Any further distribution of this work must maintain attribution to the author(s) and the title of the work, journal citation and DOI.

Keywords: High temperature Superconductor, Coated conductors, Penetration field, REBCO, CORC[®], Roebel cable, Stacked tape conductor

(Some figures may appear in colour only in the online journal)

1. Introduction

REBCO high-temperature superconductors (HTS) are a possible candidate for application in magnets for fusion, particle accelerators, and various power machines like electric motors, generators, and transmission power lines. The conductors in many of those applications will be exposed to AC magnetic fields and operate at AC currents. The AC conditions result in the generation of losses in the cables, and the operating conditions result in particular requirements for the design of the superconducting cables [1, 2]. Several different cabling designs were already demonstrated [3–10] using commercially available REBCO tapes. The tape shape brings some peculiarities in the cable design, cabling, and coil winding process and eventual operation. REBCO cables are composed of numerous individual tapes to achieve the required current capacity. The tape geometry affects the AC loss characteristics of HTS cables similar to low-temperature superconductors (LTS), mostly consisting of cables made from round strands. One such feature is the AC loss dependence on the magnetic field orientation to the wide side of the tape. For superconductors of simple shapes (slab, thin strip, thin elliptic strip) it is shown that the AC loss in an external AC field (B_a) can be generally expressed by the equation in [11]:

$$Q = S \frac{\pi}{\mu_0} \chi_0 B_a^2 \chi''_{\text{int}}(y) \quad [J] \quad (1)$$

where S is the superconductor cross-section area, $\chi''_{\text{int}}(y)$ is the imaginary part of the internal complex magnetic susceptibility, and χ_0 is a shape factor. The shape factor is roughly estimated for conductors with simple geometry [9] as:

$$\chi_0 = 1 + \frac{a}{b} \quad (2)$$

where a is the dimension perpendicular to the applied field, and b is the dimension parallel to the applied field. When the magnetic field is oriented parallel to the wide REBCO side, $\chi_0 \approx 1$ and when applied perpendicular to the wide REBCO side; $\chi_0 \gg 1$. That results in a significant hysteresis loss when the magnetic field orientation is mainly perpendicular to the wide side of the conductor. A possible solution for this issue could be striating the REBCO layer to create small superconducting filaments. It is shown [12, 13] that striating reduces the AC hysteresis loss effectively. HTS CORC[®] cables with striated tapes reduced AC loss as much as five times compared to non-striated tapes [14]. The high aspect ratio of tapes also leads to high values of the penetration field when the external magnetic field is applied perpendicular to the wide side of the tape [15]. Multi-tape REBCO conductors will also generate coupling currents between tapes that are in electrical contact, and the associated coupling loss adds to the hysteresis loss. If

the applied field is less than the penetration field, the inner layers of the conductors will be shielded by screening currents at the outer layer resulting in a significant reduction in AC coupling loss. Current sharing between tapes is essential for stability, which means that the inter-tape contact resistance (R_c) is an important parameter for multi-tape conductors. The R_c controls the coupling currents and can limit the associated coupling losses in an alternating magnetic field. The complex structure of REBCO cabled conductors makes it difficult to calculate the overall AC loss by analytical methods. Furthermore, the amount of AC loss depends on the internal geometry and material properties of the superconducting tape, the cabling geometry, and the tape-to-tape contact resistance. Although measurements of AC loss on HTS conductors have been performed [16, 17], there is a need for measurements of AC loss and contact resistance in cabled REBCO conductors.

CORC[®] cables are composed of several layers of helically wound HTS tapes on a round core with the winding direction reversed in each successive layer [18]. ENEA HTS CICC consists of stacked superconducting tapes that are placed into the helical grooves (five bundles) of an aluminum slotted core. The design, manufacturing process, and the results of critical current measurements of the HTS CICC are published in [5, 6, 19]. Extensive measurements of contact resistance and AC loss made on the Roebel cable are published elsewhere [20]. A recent study [21] on CORC[®] cable and Roebel magnetization shows that the magnetization levels measured are significantly larger than that of LTS conductors, which may lead to significant field errors.

In this work, the AC loss of eight REBCO conductor types, representing different cabling methods (CORC[®], Roebel, stacked tapes, CICC) were measured under the same conditions. The AC loss was measured without transport current and using a sinusoidal applied transverse magnetic field as a function of its frequency. The contact resistance was also measured on CORC[®], CICC, and stacked tapes conductors at temperatures of 4.2 and 77 K.

2. Experimental details

2.1. Sample layout

Different CORC[®] samples were provided by Advanced Conductor Technologies. The CORC[®]-Cu (copper-plated tapes) and CORC[®]-Sn (copper-plated tapes with solder coating) samples (figure 1) were made using an automated winding machine with SuperPower SCS4050 tapes. CORC[®]-Cu was wound from 2 copper tapes followed by 30 superconducting tapes in 13 layers around a central aluminum former of 4.2 mm diameter. The sample length is 420 mm, and the outer diameter is 6.6 mm. The CORC[®]-Sn sample was wound from 4

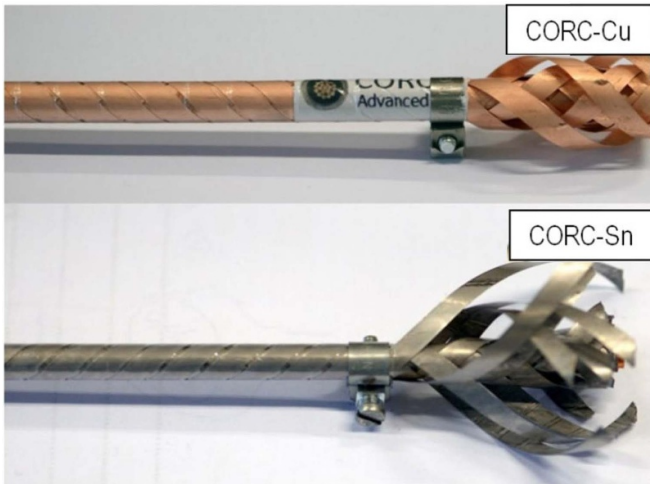


Figure 1. The CORC® conductor samples CORC®-Cu and CORC®-Sn.

copper tapes followed by 25 superconducting tapes in 12 layers around a central copper former of 4.1 mm diameter. The superconducting tapes are plated with a Pb60Sn40 alloy that has a melting temperature of ~ 180 °C. The sample length is 355 mm, with an outer diameter of 6.5 mm.

Contact resistance and AC loss measurements were done for the CORC®-Sn sample before and after the sample was heat-treated to solder the tapes together. The sample heat treatment was performed in ambient air with a maximum temperature of 210 °C. The temperature was monitored by a thermocouple attached to the central copper core. The total time of the heat treatment was 465 s with the time at which the sample was heated above 200 °C limited to 30 s. Two metal clamps were mounted at the sample ends to prevent tapes from unravelling during heat treatment. After completing the heat treatment cycle, the sample was taken out of the oven and cooled to room temperature by natural convection. Visual inspection of the sample after the heat treatment showed that soldering was successful. The layout of the CORC® conductors and selected tapes for inter-tape resistance measurements are presented in table 1.

The stacked tape conductors were made at the Swiss Plasma Centre (SPC) and Karlsruhe Institute of Technology (KIT). Two non-twisted stacked tape conductors made by SPC contain 15 SuperPower SC4050 tapes. The only difference between these two conductors is the presence of a copper shell around the stacked tapes. Figure 2 shows the conductor cross-sections. The length of the stacked tape sample without copper shell is 407 mm, and the cross-section is 4.2×1.6 mm. The conductor with copper shell has a length of 420 mm, and the outer diameter is 6.1 mm. The preparation procedure and results of critical current measurements for the conductor with copper shell is published in [4, 6].

The third stacked tape conductor with copper shell, also made by SPC, has a twist pitch of 320 mm to reduce the coupling loss. The conductor contains 16 SuperOx tapes, and the sample length is 320 mm, which is equal to one twist pitch

Table 1. The layout of the CORC® conductors and the tapes selected for the contact resistance measurement. The innermost layer is labeled as number 1.

layer #	CORC® - Cu		CORC® - Sn	
	Tape number selected for R_c	tapes in layer	tapes selected for R_c	tapes in layer
1	–	2 Cu	–	2 Cu
2	12,13	2 SC	–	2 Cu
3	10,11	2 SC	12,13	2 SC
4	–	2 SC	10,11	2 SC
5	9	2 SC	9	2 SC
6	–	2 SC	–	2 SC
7	7,8	2 SC	7,8	2 SC
8	–	3 SC	6	3 SC
9	6	3 SC	4,5	3 SC
10	4,5	3 SC	3	3 SC
11	3	3 SC	–	3 SC
12	–	3 SC	1, 2	3 SC
13	1, 2	3 SC	–	X

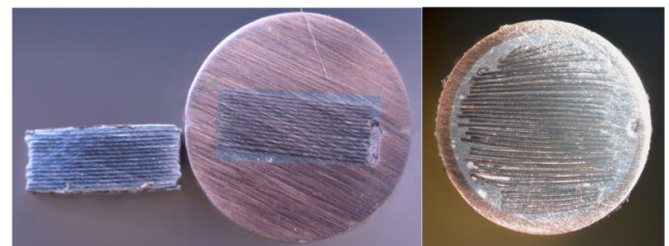


Figure 2. Cross-section of the rectangular and round stacked tape conductors, with and without copper stabilizer (left) and CroCo conductor with copper tube (right).

length. The outer conductor diameter is 6.1 mm. The cross-section of the twisted stacked conductor is similar to the one from the non-twisted stacked tape conductor with copper shell, as shown in figure 2. Details of the fabrication procedure for the twisted stacked conductor are given in [22].

The so-called CroCo conductor was prepared by KIT. It contains 22 tapes of 6 mm width, 10 tapes of 4 mm width, and is surrounded by a copper tube of 9 mm outer diameter that is filled with solder. The CroCo conductor has a twist pitch of 400 mm length, and the conductor cross-section is shown in figure 2.

A full-size prototype REBCO CICC was manufactured by ENEA. Figure 3 shows the conductor sample cross-section and schematic view of the cable layout. The conductor has five petals, each containing 18 superconducting SuNAM® tapes that are placed into the grooves of the aluminum slotted core. The specimen length is 475 mm, while the conductor twist pitch length amounts to 450 mm. The outer diameter of the conductor is 21.4 mm. A recent study [23] shows that bending of the ENEA conductor results in a decrease of the inter-tape contact resistance between neighboring tapes. This indicates

that bending or transverse load increases the current sharing between tapes by forcing the tapes towards each other. The R_c between two tapes decreases with an increase in pressure; this is in accordance with Holm's electrical contact theory [24].

The Roebel type of cable was manufactured at KIT (see figure 4) as part of the EuCARD2 collaboration. The sample was made of 15 SuperPower SCS12050 tapes that were punched into the meandering Roebel pattern. The conductor sample length is 225 mm, which is equal to one transposition length. The sample thickness is 0.8 mm, and the width is 13 mm. The conductor was vacuum impregnated with alumina-filled epoxy resin CTD-101G. The thermal contraction of the epoxy was modified by incorporating fused silica powder in order to match the thermal contraction of the REBCO tapes to prevent tape delamination during cooling down [25].

The sample properties are summarized in table 2.

2.2. Contact resistance measurements

The four-point probe method was used with a current of 10 A to measure the contact resistance (R_c) values. The R_c is defined as:

$$R_c = \frac{V}{I} \cdot l \quad [\Omega m], \quad (3)$$

where V is the measured voltage, I is the current applied through the selected tape combination, and l is the length of the sample. Special care was taken to avoid possible superconducting bridges between individual tapes at the sample ends.

For the CORC[®] conductors, R_c between tapes from the same layer and contact resistance between tapes from different layers are distinguished. The tapes from the first and last layers in CORC[®] samples have contact with only one adjacent superconducting layer. For that reason, the first and last layers (layers 2 and 13 in CORC[®]-Cu and layers 3 and 12 in CORC[®]-Sn) were chosen for R_c measurement between tapes within the same layer. Three other layers, equally distributed over the conductor depth, were chosen to measure the R_c between tapes within the same layer. The layer to layer R_c was measured between tape 13 from the first superconducting layer (layer 2 for CORC[®]-Cu and layer 3 for CORC[®]-Sn) and tape or tapes from a selected layer. Table 1 summarizes the CORC[®] conductors' layout and combinations of tapes selected for the R_c measurement.

The R_c measurements on CORC[®]-Cu were made in liquid nitrogen and liquid helium baths at 77 and 4.2 K, respectively. R_c of CORC[®]-Sn was only measured at 77 K because the Pb60Sn40 solder alloy deposited on tapes becomes superconducting at 4.2 K. Therefore, R_c measurements are not possible at this temperature unless a background magnetic field would be present.

Among stacked tape conductors, the twisted stacked tape conductor made by SPC with 16 SuperOx[®] tapes and a copper shell was selected for the R_c measurements. R_c was measured between the first tape (innermost layer) and the remaining tapes in the stack up to the outer layer. Some tapes in the middle layer are skipped due to the limited number of measuring channels in the experimental setup. R_c for the stacked tape

conductor without copper shell was measured only between the first and last tape in the stack because of the soldered tapes. Individual tapes of the measured cable were not accessible at the terminals, unlike twisted stacked tape with copper shell.

R_c measurements on the ENEA HTS CICC sample were carried out between the first, second, and the last tape from the same petal (intra-petal R_c). The average tape-to-tape resistance is calculated as R_c between first and last tape in the stack divided by the number n of contacts between tapes in the stack. The inter-petal resistances were measured between tapes from different petals. In table 3, the tape combinations for the R_c measurement in the ENEA HTS CICC sample are listed.

2.3. AC loss method

The AC loss of the sample conductors was measured in the Twente AC dipole setup, providing AC and DC magnetic field with a homogeneous field length of more than 50 cm. The AC loss measurements were carried out at 4.2 K in a liquid helium bath with a 0.4 T amplitude sinusoidal modulated magnetic field with and without an offset field of 1 T for a frequency range of 5 to 55 mHz. The AC loss was measured by gas flow calorimetry, which measures the power dissipation in the sample using gas flow measurement of the helium boil off. Simultaneously, the sample magnetization is measured by a compensated pick-up coil set [26]. The magnetization loop area is calibrated by using calorimetric data.

AC losses in CORC[®]-Cu, CORC[®]-Sn, and Roebel cables were also measured at 77 K in liquid nitrogen bath using a double wall anti-cryostat that was inserted in the AC dipole setup. The AC loss at 77 K was measured by the magnetization method only. The mutual configuration between pick up coils and the sample was kept the same for the 4.2 and 77 K measurements in order to have the same calibration factor for the measurement at 77 K. The measured AC loss is normalized by volume of superconducting tapes in the sample for each conductor. The frequency dependence of the total loss Q_{tot} per cycle allows distinguishing between hysteresis and coupling losses. The frequency-dependent part of the AC loss represents the coupling loss, while the value extrapolated to zero field frequency corresponds to the hysteresis loss Q_{hys} in a conductor.

The time required for the coupling current to decay is characterized by a coupling loss time constant, $n\tau$. A decrease in the transverse contact resistance can lead to an increase in coupling loss time constant. The time constant is a measure to compare the AC loss performance of different conductor designs. By making a fit of the AC loss frequency dependence with a linear or second-order polynomial function, the initial slope of the loss curve α and the Q_{hys} values can be obtained. The slope α then is used to calculate the coupling loss time constant $n\tau$ [27] using the formula:

$$n\tau = \alpha \frac{\mu_0}{2\pi^2 B_a^2} \quad [s] \quad (4)$$

The total AC loss of the CORC[®]-Cu, CORC[®]-Sn, and Roebel cables was also measured as a function of applied magnetic field amplitude at 4.2 K in order to find the penetration

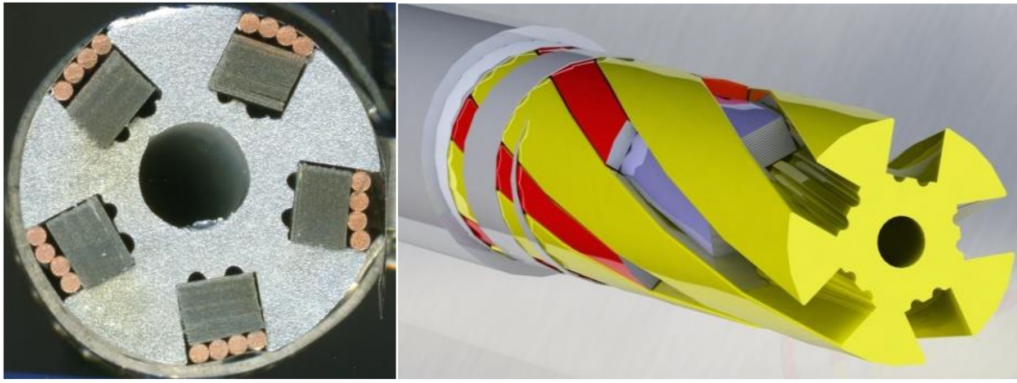


Figure 3. Cross-section and schematic view of ENEA HTS CICC.



Figure 4. The structure of the impregnated Roebel cable.

Table 2. Summary of REBCO cable sample properties.

Sample name	Tape manufacturer	Number of tapes	Sample dimensions $l \times w \times h$ or $l \times d$ (mm)	The volume of SC tapes in the sample (cm ³)	Twist pitch or transposition length (mm)	Sample I_c at 77 K, self field (A)
Stacked conductor with Cu shell	SuperPower	15	420 × d6.1	3.3	non-twisted	~1100 A ^b
Stacked conductor without Cu shell	SuperPower	15	407 × 4.2 × 1.6	2.9	non-twisted	~1100 A ^b
Twisted Stacked conductor with Cu Shell	SuperOX	16	320 × d6.1	2.6	320	~1580 A ^b
HTS CICC	SuNam	90	475 × d21.4	25.5	450	~13 000 A ^b
Roebel cable	SuperPower	15	225 × 13 × 0.8	2.9	225	~2600 A ^b
CORC [®] -Cu	SuperPower	30	420 × d6.6	7.1	12.1–23.0 ^a	1900 A ^b
CORC [®] -Sn	SuperPower	25	355 × d6.5	5.3	12.1–23.0 ^a	1650 A ^b
CORC [®] -Sn after HT	SuperPower	25	355 × d6.5	5.3	12.1–23.0 ^a	1650 A ^b
CroCO	SuperPower	32	400 × d7.0	4.7	400	~3150 A ^b

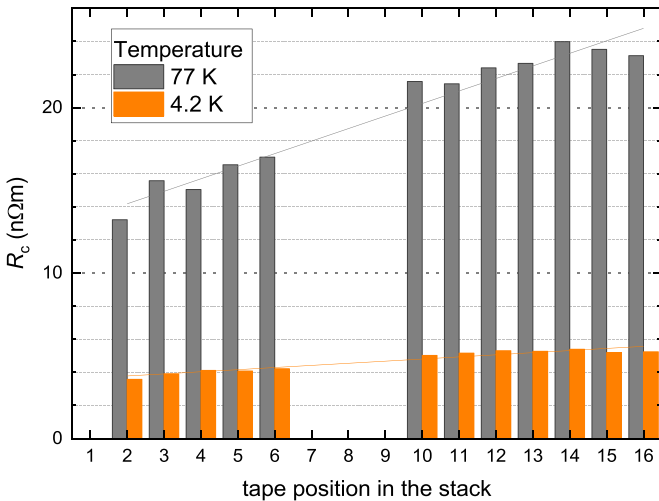
atwist pitch length varies for different layers,^b I_c is estimated.

field. During that measurement, the magnetic field frequency was kept constant at 10 mHz, while the amplitude of the magnetic field was varied from 10 to 1500 mT. For the Roebel cable, the measurement was also done at 77 K.

The AC loss was also measured on CORC[®] conductors at 4.2 K with the applied magnetic field orientation parallel with the sample length axis by using an AC solenoid magnet.

Table 3. Tape combinations for the contact resistance measurements on the ENEA HTS CICC.

Petal #	Contact number	Corresponding tape number in petal
1	R1, R2, R3.	1, 9, 18
2	R4, R5, R6	1, 2, 18
3	R7, R8, R9.	1, 2, 18
4	R10, R11, R12.	1, 2, 18

**Figure 5.** Measured R_c between tapes in the twisted stacked sample with Cu shell.

3. Results and discussion

3.1. Contact resistance results

3.1.1. Stacked tape conductors contact resistance. Figure 5 shows contact resistances for the twisted stacked tape conductor with copper shell. At 77 K, the R_c between tapes varies from 13 nΩm for neighboring tapes up to 24 nΩm between the first tape and tape number 14. At 4.2 K, R_c decreases to 3.5 nΩm for the neighboring tapes and 5.4 nΩm between tape 1 and tape 14. These values correspond to an average increase of 0.75 nΩm/layer and 0.12 nΩm/layer of R_c between adjacent tapes from innermost to outermost layer at 77 and 4.2 K respectively

R_c of the stacked tape conductor without copper shell was measured to determine the influence of the copper shell on R_c . For the conductor without copper shell, the R_c measurement was possible only between the first and last tape (number 15) in the stack, giving 199 nΩm at 77 K and 32 nΩm at 4.2 K.

The conductor without copper shell has an order of magnitude higher R_c values between innermost and outermost tapes as compared to the conductor with copper shell. R_c measurements were not carried out on the untwisted stacked tape with copper shell. While the influence of twisting on AC coupling loss should be significant, the influence of twisting on R_c expected to be minimal.

Lower R_c between distant tapes for the twisted stacked tape conductor with copper shell compared to the sample

Table 4. Tape to tape contact resistance for CORC[®]-Cu at 4.2 and 77 K for tapes within the same layer.

	R_c at 77 K (nΩm)	R_c at 4.2 K (nΩm)	R_c difference between 77 and 4.2 K (%)
layer 2	6860	13 030	+90
layer 3	1070	1030	-4
layer 7	980	782	-20
layer 10	1110	832	-25
layer 13	3890	2760	-29

without copper shell indicates that current sharing between tapes mostly takes place through the copper shell rather than through the stack of tapes. That conclusion is supported by R_c measurements at 4.2 K. Figure 5 shows that R_c between the first and any corresponding tape is almost independent on the position of the tape in the stack at 4.2 K. That observation confirms that tapes are effectively coupled via the low resistive copper shell.

3.1.2. Contact resistance of CORC[®]-Cu conductor. R_c values measured between two tapes from the same layer of the CORC[®]-Cu sample are presented in table 4. The tapes within the same layer are not in physical contact with one another. R_c measured within internal layers 3, 7, and 10 is in the same order of magnitude, while R_c measured within layers 2 and 13 are significantly higher because those layers are only in direct contact with one neighboring superconducting layer. Upon cooling down from 77 to 4.2 K, R_c decreases for all layers except layer 2. Layer 2 shows an R_c increase from 6860 to 13 030 nΩm, which may be explained by the CORC[®]-Cu conductor layout. The central former of the CORC[®]-Cu is made of an aluminum rod that has a coefficient of thermal expansion of $2.3 \times 10^{-5} \text{ K}^{-1}$ [28] while the Hastelloy based REBCO tapes have a smaller thermal expansion coefficient of $1.12 \times 10^{-5} \text{ K}^{-1}$ [29]. The REBCO tapes from layer 2 lose their pre-tension applied during conductor manufacturing upon cooling down due to the difference in thermal expansion coefficients between the core and REBCO tapes, thus causing the increase in R_c .

The high thermal expansion coefficient of the aluminum core also results in a tension gradient across the tape layers upon conductor cooling down. The percentage of R_c change therefore depends on the layer number during cooling down. R_c differences listed in table 4 show a higher decrease in R_c during cooling down from 77 to 4.2 K in the outer layers. The relatively high thermal expansion of the polyester insulation on the outside of the cable also plays a role in the value of R_c difference.

Figure 6 presents the results of layer to layer R_c measurements for the CORC[®]-Cu sample. R_c was measured between tape 13 from layer 2 and tapes from other layers (see table 1). From the measured data, an average R_c is determined for tapes between neighboring layers (this R_c value corresponds

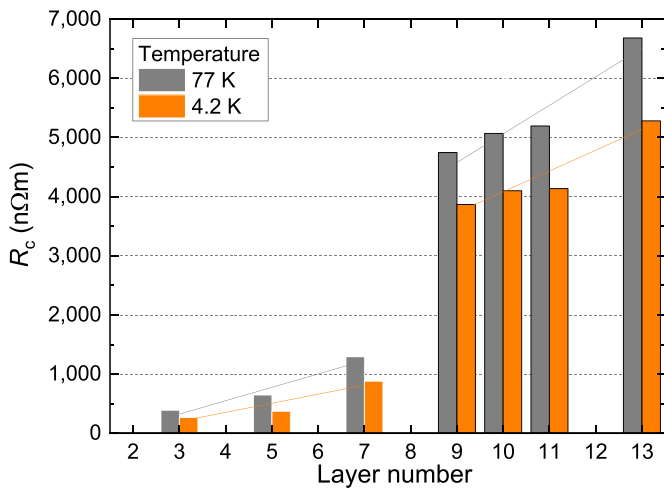


Figure 6. Layer to layer R_c between layer 2 and other layers for the CORC®-Cu sample.

Table 5. R_c between pairs of tapes within the same layer, before and after conductor heat treatment of the CORC®-Sn sample.

	R_c before HT at 77 K (nΩm)	R_c after HT at 77 K (nΩm)
layer 3	3350	10
layer 4	1670	19
layer 7	3550	28
layer 9	2650	20
layer 12	11 200	46

to R_c between neighboring tapes in stacked tape conductors). The average increase of R_c between adjacent layers is ~ 300 nΩm/layer at 77 K and ~ 230 nΩm/layer at 4.2 K. The R_c between layers 7 and 8 was excluded from these averages because a step increase in the R_c was observed between layers 7 and 9. This step increase in R_c corresponds to a change in cabling pattern between layers containing 2 tapes per layer to the layers that accommodate 3 tapes per layer (table 1). With such a transition in cabling geometry, the contact area between a tape from layer 7 and tape from layer 8 becomes smaller, which results in a higher R_c .

3.1.3. Contact resistance of CORC®-Sn conductor. Table 5 shows the results of R_c measurements between tapes from the same layer before and after the conductor heat treatment. Before the heat treatment, R_c between tapes from the same layer varies from 1670 to 11 200 nΩm with an average value of 4480 nΩm. R_c decreased by two orders of magnitude after the sample conductor was heat-treated and varied from 9.5 to 46 nΩm. The observed decrease in R_c is an indication of successful tape-to-tape soldering in the CORC®-Sn sample. The fact that all layers showed a similar decrease in R_c between tapes within the same layer indicate that soldering took place homogeneously along the entire conductor volume.

The CORC®-Sn sample layer-to-layer R_c is shown in figure 7. The layer-to-layer R_c was measured between tape 13 from layer 3 and tapes from the other layers (see table 1). The

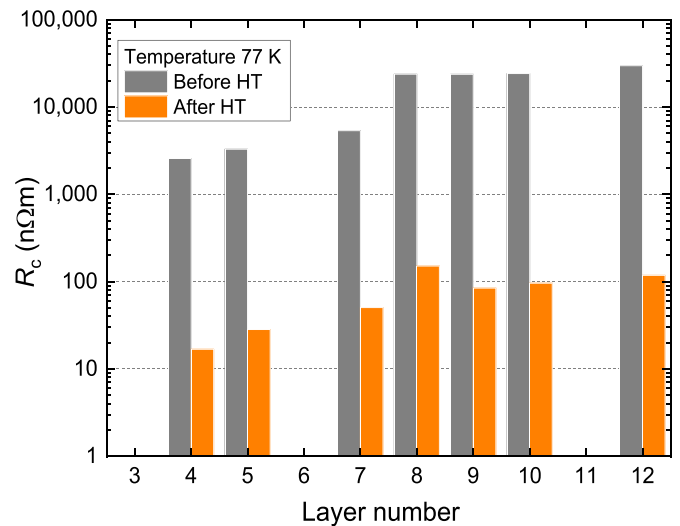


Figure 7. Layer to layer R_c measured between layer 3 and other layers before and after the conductor soldering heat treatment of the CORC®-Sn sample.

average increase of R_c from innermost (~ 2600 nΩm) to outermost layer ($\sim 30\,000$ nΩm) amounts to ~ 3900 nΩm/layer at 77 K before heat treatment. Similar to the CORC®-Cu results, a step increase in the contact resistance was observed between layer 7 and layer 8 corresponding with the transition in cabling pattern between layers containing 2 tapes per layer to layers with 3 tapes (table 1). The heat treatment decreased R_c by two orders of magnitude, as illustrated in figure 7, with an average increase of R_c from innermost (~ 16 nΩm) to the outermost layer (~ 120 nΩm) of ~ 13 nΩm/layer at 77 K.

It can be noted that layer-to-layer R_c for the CORC®-Cu and CORC®-Sn sample before heat treatment, are in the same order of magnitude and the difference in surface material does not strongly affect the R_c . It may be expected that in analogy with the classical NbTi and Nb₃Sn cabled conductors, in particular, when considering the effect of the heat treatment on the CORC®-Sn R_c , that the surface oxide layer is mostly determining the R_c [30–34]. This means that a heat treatment or mechanical cycling [35] alter the R_c significantly. A recent study [36] on R_c of REBCO tapes shows that R_c decreased to about one tenth of its initial value after 1000 cycles.

3.2. HTS Cable in conduit conductor contact resistance

Table 6 shows R_c values between neighboring tapes in petals for the ENEA HTS CICC sample. The average R_c between adjacent tapes is in a range of 360 nΩm at 77 K. After the conductor was cooled down further to 4.2 K, R_c between adjacent tapes decreased to ~ 180 nΩm. Measured values are in very good agreement with layer-to-layer R_c measured on the CORC®-Cu conductor. This suggests that the tape manufacturer or cable pattern may not play a significant role in the tape to tape R_c for copper-plated tapes in cables. Further experiments are required on the effect of cabling tension and contact area of HTS cables to confirm the above the statement.

Table 6. The measured R_c between neighboring tapes for the HTS CICC sample.

	R_c at 77 K (nΩm)	R_c at 4.2 K (nΩm)	R_c difference between 77 and 4.2 K (%)
layer 1	380	240	−37
layer 2	340	120	−65
layer 3	340	160	−53
layer 4	370	190	−49

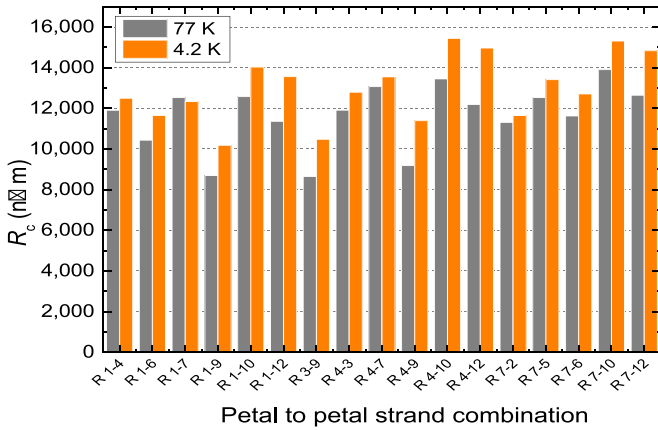


Figure 8. Inter-petal R_c for the HTS CICC conductor sample.

The inter-petal resistance results are presented in figure 8 as a function of the selected tapes. The average petal-to-petal R_c is around 11 000 nΩm at 77 K. Almost all tape combinations showed a moderate increase in the inter-petal resistance upon sample cool-down from 77 to 4.2 K. The average inter-petal R_c increases to 13 000 nΩm at 4.2 K, this is an order of magnitude higher compared with inter-petal resistance found for full-size ITER NbTi and Nb₃Sn conductors [35, 37]. The increase of R_c upon cool-down from 77 K to 4.2 K is likely due to the larger coefficient of thermal expansion of the Aluminum core, as discussed in section 3.1.2. The high level of inter petal resistance practically excludes significant current sharing between petals in the HTS CICC conductor sample. However, it should be noted that no electromagnetic load is involved in this test. Applying a transverse load may reduce intra- and inter-petal R_c .

3.3. AC loss of CORC[®]-Cu, CORC[®]-Sn, and Roebel cable at 4.2 K

Figure 9 shows the total AC loss versus frequency of the applied magnetic field for the CORC[®]-Cu, heat-treated CORC[®]-Sn, and Roebel cables. The AC loss data of the Roebel cable in figure 9 is presented for the magnetic field perpendicular to the wide side of the conductor. The AC loss is frequency independent for all conductors. That implies that the hysteresis loss is the dominant loss in the conductors at a given temperature, AC superposed field amplitude, and conductor to field orientation. When the background offset field

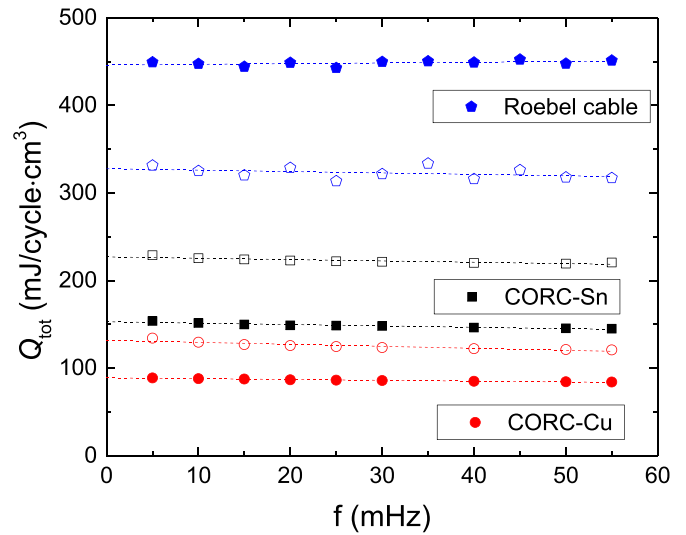


Figure 9. AC loss of CORC[®] and Roebel conductors at zero and 1 T background magnetic field. Filled symbols represent the measurement data without background field; open symbols measurement with 1 T background field at 4.2 K. The magnetic field is oriented perpendicular to the wide conductor side.

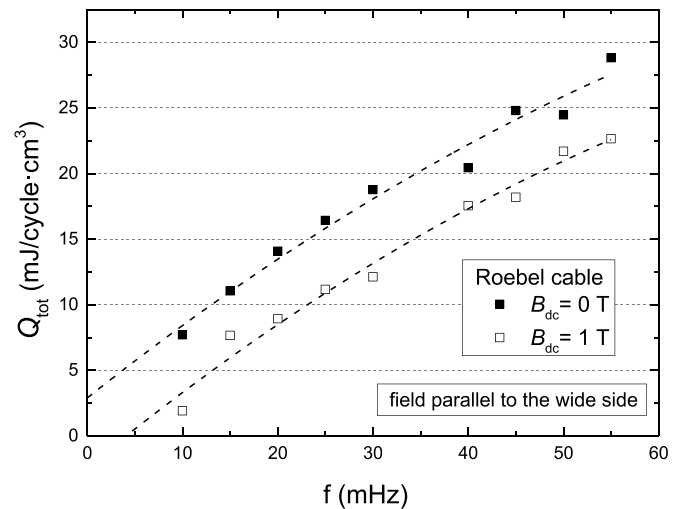


Figure 10. AC loss of the Roebel cable versus frequency at 4.2 K. The magnetic field is oriented parallel to the wide conductor side.

of $B_{dc} = 1$ T is applied, the AC loss of both CORC[®] conductors increases. This AC loss behavior is opposite to what is commonly observed for low-temperature superconductors (LTS), where the AC loss decreases when a background field is applied. The AC loss decrease in LTS is explained by the decrease of the critical current density (J_c) when the background magnetic field is increased. The increase of AC loss with the background field indicates that there are additional eddy current losses associated with the core of CORC[®] cables. At low fields, the loss contribution from the conductor core can exceed the losses from the rest of the entire cable as reported in [38].

The AC loss of the CORC[®]-Sn conductor was measured before and after the heat treatment. Even though the contact resistance lowered to tens of nΩm between neighboring tapes

and layers (see section 3.1.3), no coupling loss was observed for the heat-treated CORC[®]-Sn conductor. This is a strong indication that the wide REBCO tapes, representing a large effective filament diameter, are not fully penetrated, and the outer layer of the cable shields the inner layers of the conductor from external applied field. A recent study shows that with increase in the number of cable layers the cable losses per tape decreases due to shielding effects [39]. The shielding effect also increases with the HTS tape coverage ratio on the cable [24]. Virtually, no influence of the CORC[®]-Sn heat treatment on the coupling loss was observed. An interesting observation is that the CORC[®]-Sn conductor seems to have significantly higher hysteresis loss than the CORC[®]-Cu sample though the CORC[®]-Sn sample is made of 25 tapes while the CORC[®]-Cu is made of 30 tapes. The elevated Q_h of CORC[®]-Sn can be partly a consequence of the lower tape twist angle but more likely is the contribution of the superconducting solder coating to the hysteresis loss.

AC loss of the Roebel conductor with field applied perpendicular to the tape is also frequency independent and becomes less with applied background magnetic field (figure 9). However, when the magnetic field is oriented parallel to the wide side of the Roebel conductor (figure 10), the loss-frequency dependence shows the characteristic behavior of coupling loss in an alternating magnetic field. The coupling loss time constants are summarized in table 9. The magnetization response from the Roebel conductor is low for the magnetic field oriented parallel to the wide REBCO side. The low level of AC loss generation makes the calorimetric AC loss measurement less accurate and, as a result, makes magnetization loop calibration not very precise. Hence, the AC loss values of the Roebel cable in this field orientation should be treated as an estimation only. The goal of the measurement in parallel field orientation is to confirm the presence of AC coupling currents between tapes in a Roebel cable.

3.4. Penetration field estimation

The apparent absence of AC coupling loss in the CORC[®] conductors under applied conditions (0.4 T amplitude sinusoidal modulated magnetic field with and without offset field of 1 T for a frequency range of 5 to 55 mHz) is most likely because the wide filaments with high J_c are not fully penetrated. The screening currents in the outer layer of tapes are entirely shielding the inner conductor part from the applied magnetic field. The penetration field for a single REBCO tape in the case of a field applied perpendicular to the wide side of the tape, as a superconducting thin strip, is given by formula in [15],

$$B_p \approx \mu_0 J_c \left(\frac{2t}{\pi} \right) \left(\ln \frac{2w}{t} \right) \quad [\text{T}] \quad (5)$$

where J_c is the critical current density of the superconductor, t is the half-thickness of the superconductor, and w is the half-width. J_c of $\sim 2.2 \times 10^5$ A mm⁻² in self-field at 4.2 K and $\sim 1.3 \times 10^4$ A mm⁻² at 77 K was estimated from [40] while w and t are 2 mm and 0.8 μm , respectively for SCS4050 tape

Table 7. AC coupling loss time constants of CORC[®]-Sn and CORC[®]-Cu samples in a parallel magnetic field. The Q_{hys} values are indicative and only to illustrate that they are negligible compared to the coupling loss.

	CORC [®] -Sn	CORC [®] -Cu
$n\tau$ (ms), $B_a = \pm 0.4$ T	$27\,400 \pm 4700$	788 ± 16
$n\tau$ (ms), $B_a = 0.6\text{--}1.4$ T	$25\,200 \pm 500$	763 ± 5
Q_{hys} (mJ/cycle.cm ³)	2.5 ± 3.4	-1.5 ± 1.6

with 1.6 μm REBCO layer thickness. That gives a penetration field of $B_p \approx 1200$ mT at 4.2 K and $B_p \approx 70$ mT at 77 K.

For the magnetic field applied parallel to the wide surface of the REBCO tape (infinite length), the penetration field of a slab is given by [41]:

$$B_p \approx \mu_0 J_c t \quad [\text{T}] \quad (6)$$

For $t = 0.8$ μm , the penetration field amounts to $B_p \approx 220$ mT at 4.2 K and $B_p \approx 13$ mT at 77 K.

The estimated penetration field values suggest that under applied conditions the internal part of CORC[®] conductors is shielded from the magnetic field entirely by screening currents in the outermost layer of tapes.

In order to assess the conductors' penetration fields experimentally, the total AC loss is measured as a function of applied magnetic field amplitude. Figure 11 shows Q_{tot} divided by the square of the applied field amplitude (B_{apl}) as a function of the field amplitude. The saturation of AC loss occurs around an amplitude of the applied field of ~ 1 T for the Roebel and CORC[®]-Sn conductors, while saturation of CORC[®]-Cu occurs at a higher field of ~ 1.3 T. The saturation values measured experimentally are in good agreement with our estimation of the penetration field at 4.2 K. The CroCO conductor represents the configuration of twisted stack conductors with a saturation peak at 40 mT and likely a peak at higher applied field amplitude. The saturation at 40 mT corresponds well to the field penetration at the area of the conductor, where tapes are parallel to the applied field.

For the Roebel cable, the same measurement was performed in a liquid nitrogen bath at 77 K, and the results in figure 11 show that the AC loss saturation occurs at ~ 70 mT. The estimation of the penetration field values together with experimental measurements show that hysteresis loss is the dominant loss in REBCO cables at 4.2 K when the magnetic field is oriented perpendicular to the wide side of the REBCO tape and the amplitude of the magnetic field is below 1 T. At the chosen amplitude and magnetic field orientation, the AC coupling loss should indeed be negligible at 4.2 K since the measurements are done below the penetration field, and the interior layers are fully shielded.

In order to further evaluate the penetration field effects, the total AC loss of the CORC[®] conductors was measured with the AC magnetic field oriented parallel to the longitudinal conductor axis. Also, the total AC loss of the CORC[®] and Roebel cables were measured in the transverse magnetic field at a liquid nitrogen bath temperature

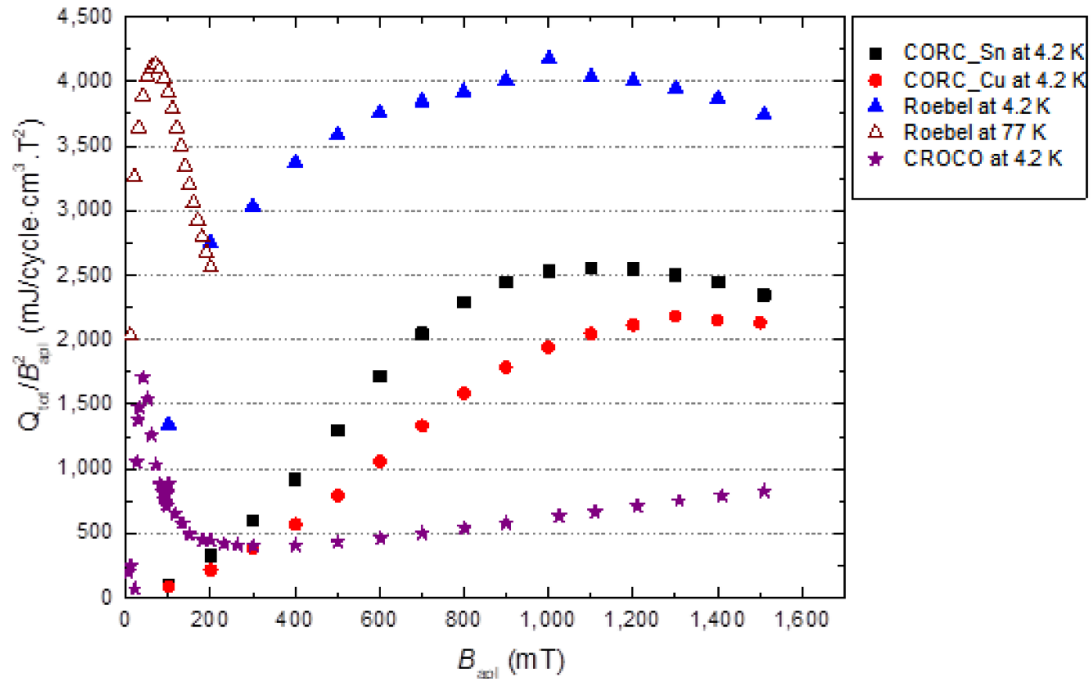


Figure 11. Total AC loss divided by the square of the magnetic field amplitude versus the amplitude of the applied field. Measurements are done at 10 mHz magnetic field frequency. The magnetic field is oriented perpendicular to the conductor axis (field perpendicular to the wide side of conductor for Roebel cable).

Table 8. Hysteresis loss and coupling time constants measured at 77 K.

	Number of tapes	Volume of SC tapes in sample (cm ³)	B _d = 0 T	Coupling loss time constant nτ, (ms)		Hysteresis loss Q _h (mJ/cycle.cm ³)
				B _d = 1 T	B _d = 0 T	B _d = 1 T
Roebel cable ^a	15	2.9	154 ± 7	87 ± 4	179 ± 1	108 ± 1
CORC [®] -Cu	30	7.1	82 ± 4	32 ± 4	284 ± 1	124 ± 1
CORC [®] -Sn	25	5.3	483 ± 14	258 ± 21	296 ± 1	105 ± 2

after HT

afield perpendicular to the wide side

Table 9. Sample AC loss parameters measured at 4.2 K.

Sample name	Coupling time constant nτ, (ms)		Hysteresis loss Q _h (mJ/cycle.cm ³)			
	B _d = 0 T	B _d = 1 T	field parallel to the wide side		field perpendicular to the wide side	
			B _d = 0 T	B _d = 1 T	B _d = 0 T	B _d = 1 T
Stacked conductor, CU	2634 ± 29	2345 ± 18	4 ± 1	5 ± 1	102 ± 1	96 ± 1
Stacked conductor	140	111	1 ± 1	3 ± 1	97 ± 1	91 ± 1
Stacked conductor CU-twisted	360 ± 2	279 ± 2	40 ± 1	41 ± 1	–	–
HTS CICC	126 ± 10	115 ± 3	45 ± 1	51 ± 2	–	–
Roebel cable	255 ± 51	249 ± 71	2 ± 2	–	447 ± 2	328 ± 4
CORC [®] -Cu	–	–	–	–	89 ± 1	132 ± 1
CORC [®] -Sn	–	–	–	–	153 ± 1	227 ± 1
CORC [®] -Sn after HT	–	–	–	–	158 ± 1	243 ± 2
CroCO	1039 ± 8	1087 ± 13	37 ± 1	36 ± 1	–	–

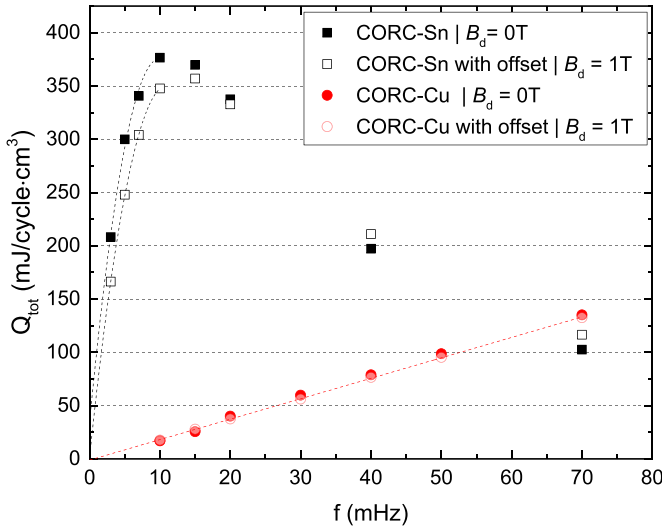


Figure 12. AC loss of the CORC[®] conductors at 4.2 K for the magnetic field applied parallel to the conductor length axis. Dashed lines are curves fit to the experimental data.

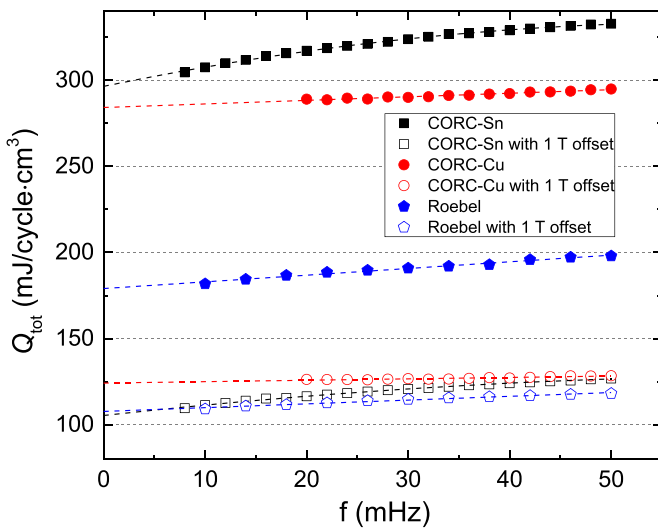


Figure 13. AC loss of the CORC[®] and Roebel conductors at 77 K in a transverse applied field, with and without offset field of 1 T. Dashed lines are linear and polynomial fits.

3.5. AC loss of CORC[®] conductors in a parallel magnetic field

The penetration field is ~ 220 mT at 4.2 K when the magnetic field is oriented parallel to the wide side of the REBCO tape according to the estimation performed using equation (6) in section 3.4. For the chosen amplitude of the AC magnetic field of 0.4 T, AC coupling currents are expected in CORC[®] samples. For confirmation, the AC loss of the CORC[®]-Cu and heat-treated CORC[®]-Sn conductors were measured using an AC solenoid magnet.

Figure 12 shows the AC loss frequency dependence of the CORC[®]-Cu and heat-treated CORC[®]-Sn conductors measured in parallel applied field with and without a background field of 1 T. The AC loss of both conductors is frequency dependant with highest coupling loss for the CORC[®]-Sn

sample showing a peak at 10 mHz. The high coupling loss can be explained by the very low resistance between the tapes leading to large coupling currents. To find the initial slope of the CORC[®]-Sn loss-frequency dependence, only data points below the AC loss peak were used to produce a second-order polynomial fit. The AC loss-frequency dependence of the CORC[®]-Cu was fit by a linear function. Table 7 presents the coupling loss time constants and Q_{hys} values calculated from the loss frequency dependence. The Q_{hys} values are relatively close to zero for both conductors, regardless of B_d . No influence of the magnetic field background is observed for the CORC[®]-Cu sample, while the AC loss of the CORC[®]-Sn sample is lower with the background field. Such AC loss behavior as observed for CORC[®]-Sn is similar to that found for LTS conductors and might be due to a combination of (1) a decrease in J_c , (2) an increase of the magnetoresistance, (3) fully normal state of the solder, as a result of the applied background magnetic field.

3.5.1. AC loss of CORC[®]-Cu, CORC[®]-Sn, and Roebel cable at 77 K in a transverse magnetic field. AC loss measurements of CORC[®]-Cu, heat-treated CORC[®]-Sn, and Roebel samples were repeated at 77 K with a magnetic field applied transverse to the samples. For the Roebel cable, the magnetic field orientation was perpendicular to the wide side of the conductor. Figure 13 shows the measured loss frequency dependence of the conductors at 77 K. AC loss becomes frequency-dependent for all measured conductors. All CORC[®] conductors show a considerable decrease in AC loss when the background field of 1 T is applied. This behavior is opposite to what was observed for the measurements done at 4.2 K in the transverse magnetic field. The decrease of AC loss can be explained by the reduction of the tape J_c in a background magnetic field. The loss frequency dependence of the CORC[®]-Cu and Roebel cables was fit by linear functions, while for CORC[®]-Sn, a second-order polynomial function was used. Table 8 lists the coupling loss time constants and hysteresis loss values of CORC[®] and Roebel conductors measured at 77 K.

3.6. AC loss of HTS CICC and stacked tape conductors

Figure 14 presents AC loss data comparison for stacked tape conductors with and without twist, CroCO, and the HTS CICC conductor. The orientation of the applied magnetic field on the non-twisted stacked tape conductors is parallel to the wide side of the REBCO conductors. Coupling loss is clearly observed for all conductors at that field orientation. The non-twisted conductor with Cu shell has the highest coupling loss among that group of the conductors. In section 3, it was shown that tapes are effectively coupled via the copper shell. The low contact resistance between tapes and the absence of tape twist leads to high coupling currents and associated loss. At the same conditions, the stacked tape conductor without Cu shell shows moderate coupling loss, while the hysteresis losses are practically the same for the conductor with and without Cu shell, see table 9. The twisted stack conductor with Cu shell shows that twisting effectively reduces the influence of tape

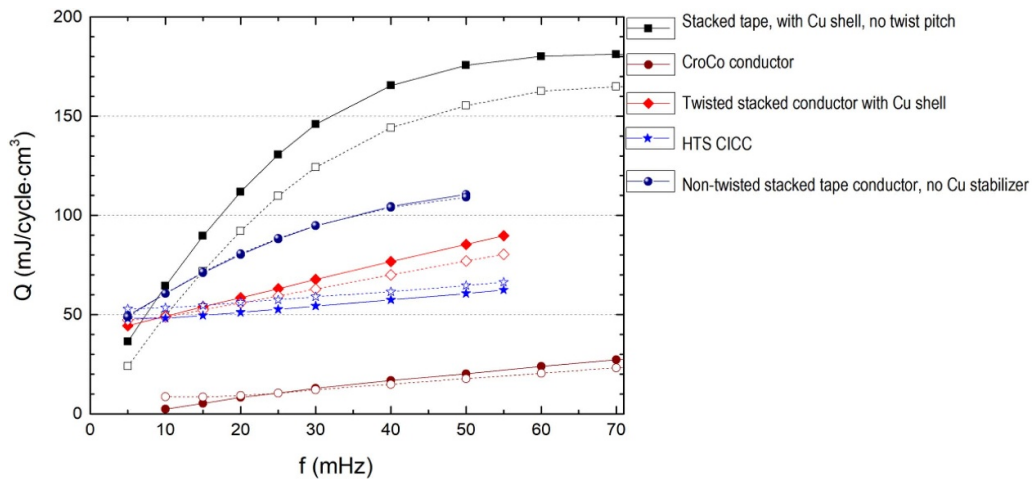


Figure 14. AC loss frequency dependence of several HTS conductors at 4.2 K. For the non-twisted stacked tape conductors, the magnetic field is oriented parallel to the wide side of the tape. The filled symbols represent the $B_d = 0$ T data, and the open symbols represent data for $B_d = 1$ T background field.

coupling via the copper shell. However, the penalty is the higher hysteresis loss compared with the non-twisted conductor. The HTS CICC conductor showed the lowest coupling losses, which can be explained by relatively high tape to tape contact resistance compared with the stacked conductors where tapes are soldered together. Modeling and AC loss calculation reported in [42] indicate that the expected AC loss from CroCo cables is higher than that of conventional concentric tape arrangements like CORC[®] cables.

The loss-frequency dependencies shown in figure 14 were fitted by a linear function or a second-order polynomial function by the least-square method. The calculated coupling loss time constants and hysteresis losses are summarized in table 9.

AC loss measurements in non-twisted stacked tape samples with the magnetic field oriented perpendicular to the wide side of the REBCO tapes show no evidence of AC coupling loss at the applied AC field of 0.4 T. The reason AC coupling losses are absent is discussed in section 3.3. The hysteresis losses dominate when the field orientation is perpendicular to the wide side of the REBCO tapes. The hysteresis loss values for stacked conductors with and without Cu shell are similar and are given in table 9.

4. Conclusion

The AC loss and inter-tape contact resistances from REBCO cables made by different cabling methods (CORC[®], stacked tape conductors, Roebel cable, and HTS CICC) were measured and compared. As a consequence of the high aspect ratio of the HTS tapes, all non-twisted conductors and the Roebel cable have high hysteresis loss in an alternating magnetic field oriented perpendicular to the wide side of the REBCO layer.

The measurements show that the coupling component of the AC loss is negligible for CORC[®] and Roebel type conductors when they are subjected to a transverse alternating magnetic field with amplitudes below the penetration field. The AC

coupling losses in CORC[®] and Roebel cables can be identified when the applied AC field amplitude exceeds the penetration field. Here the penetration field is reduced by measuring the AC loss in liquid nitrogen bath at 77 K. For twisted stacked conductors, the penetration field varies along the length of the conductor, illustrating that for AC loss analysis, the highest penetration field should be taken as a minimum limit for the applied field amplitude.

A copper shell around a stacked tape conductor provides good current sharing between all layers of tapes. The highest coupling loss among the stacked conductors was measured for the non-twisted stacked tape conductor with copper shell. When twisting is applied to a stacked tape conductor with copper shell, the coupling loss is effectively reduced at the cost of increased hysteresis loss.

Tape-to-tape contact resistances of CORC[®] and HTS CICC samples were measured as well. It was shown that contact resistances for conductors made of copper-plated REBCO tapes (HTS CICC and CORC[®]-Cu) are in the range of ~ 300 n Ω m at 77 K and ~ 200 n Ω m at 4.2 K. A step increase in contact resistance was observed for CORC[®] samples between layers, attributed to a change in the contact area when the number of tapes per layer changes from two to three. CTE mismatch between tapes within the CORC[®] conductors and an aluminum core was also found to influence the contact resistances between tapes. A CORC[®] cable with PbSn plated tapes had two times higher layer to layer contact resistance compared to the CORC[®] cable with standard copper plated tapes. However, a heat treatment to melt the solder between tapes effectively reduced the tape-to-tape and layer-to-layer contact resistances by two orders of magnitude.

Acknowledgments

This work has been carried out within the framework of the EUROfusion Consortium and has received funding from the

Euratom research and training program 2014–2018 and 2019–2020 under grant agreement No 633053. The views and opinions expressed herein do not necessarily reflect those of the European Commission. Part of the work is supported by the University of Twente, Enschede, The Netherlands. Part of the work this also supported by the U.S. Department of Energy under contract numbers DE-SC0014009 and DE-SC0015775. Also supported by the Air Force Office of Scientific Research (AFOSR) LRIR #14RQ08COR, and the Aerospace Systems Directorate (AFRL/RQ) and by the Air Force Office of Scientific Research (AFOSR) LRIR # 18RQCOR100, and the Aerospace Systems Directorate (AFRL/RQ). The views and opinions expressed herein do not necessarily reflect those of any of the above-acknowledged parties. We thank our colleagues from SPC, Villigen, Switzerland, KIT, Karlsruhe, Germany and ENEA, Frascati Research Center, Frascati, Italy, for making available the conductor samples.

ORCID iDs

V A Anvar  <https://orcid.org/0000-0003-1264-6442>

D C Van Der Laan  <https://orcid.org/0000-0001-5889-3751>

J D Weiss  <https://orcid.org/0000-0003-0026-3049>

M S A Hossain  <https://orcid.org/0000-0002-5588-0354>

A Nijhuis  <https://orcid.org/0000-0002-1600-9451>

References

- [1] Melhem Z 2011 *High Temperature Superconductors (HTS) for Energy Applications* (Cambridge: Woodhead Publishing)
- [2] Bruzzone P, Sedlak K and Stepanov B 2013 High current superconductors for DEMO *Fusion Eng. Des.* **88** 1564–8
- [3] Uglietti D, Wesche R and Bruzzone P 2014 Design and strand tests of a fusion cable composed of coated conductor tapes *IEEE Trans. Appl. Supercond.* **24** 1–4
- [4] Uglietti D, Wesche R and Bruzzone P 2013 Fabrication trials of round strands composed of coated conductor tapes *IEEE Trans. Appl. Supercond.* **23** 4802104–4802104
- [5] Augieri A *et al* 2015 Electrical characterization of ENEA high temperature superconducting cable *IEEE Trans. Appl. Supercond.* **25** 1–4
- [6] Celentano G, De Marzi G, Fabbri F, Muzzi L, Tomassetti G, Anemona A, Chiarelli S, Seri M, Bragagni A and Corte Della A 2014 Design of an industrially feasible twisted-stack HTS cable-in-conduit conductor for fusion application *IEEE Trans. Appl. Supercond.* **24** 1–5
- [7] Goldacker W, Frank A, Heller R, Schlachter S I, Ringsdorf B, Weiss K-P, Schmidt C and Schuller S 2007 ROEBEL assembled coated conductors (RACC): preparation, properties and progress *IEEE Trans. Appl. Supercond.* **17** 3398–401
- [8] Van Der Laan D C 2009 YBa₂Cu₃O_{7-??} coated conductor cabling for low ac-loss and high-field magnet applications *Supercond. Sci. Technol.* **22** 065013
- [9] Wolf M J, Fietz W H, Bayer C M, Schlachter S I, Heller R and Weiss K-P 2016 HTS CroCo: A stacked HTS conductor optimized for high currents and long-length production *IEEE Trans. Appl. Supercond.* **26** 19–24
- [10] van der Laan D C, Weiss J D and McRae D M 2019 Status of CORC® cables and wires for use in high-field magnets and power systems a decade after their introduction *Supercond. Sci. Technol.* **32** 033001
- [11] Gömöry F *et al* 2006 Predicting AC loss in practical superconductors *Supercond. Sci. Technol.* **19** S60–6
- [12] Cobb C B, Barnes P N, Haugan T J, Tolliver J, Lee E, Sumption M, Collings E and Oberly C E 2002 Hysteretic loss reduction in striated YBCO *Phys. C Supercond.* **382** 52–56
- [13] Šouc J, Gömöry F, Kováč J, Nast R, Jung A, Vojenčiak M, Grilli F and Goldacker W 2013 Low AC loss cable produced from transposed striated CC tapes *Supercond. Sci. Technol.* **26** 075020
- [14] Vojenčiak M, Kario A, Ringsdorf B, Nast R, van der Laan D C, Scheiter J, Jung A, Runtsch B, Gömöry F and Goldacker W 2015 Magnetization ac loss reduction in HTS CORC® cables made of striated coated conductors *Supercond. Sci. Technol.* **28** 104006
- [15] Brandt E H 1996 Superconductors of finite thickness in a perpendicular magnetic field: strips and slabs *Phys. Rev. B* **54** 4246–64
- [16] Solovyov M, Ouc J, Gömöry F, Šouc J and Gömöry F 2014 AC loss properties of single-layer CORC cables *J. Phys. Conf. Ser.* **507** 022034
- [17] Majoros M, Sumption M D, Collings E W and van der Laan D C 2014 Magnetization losses in superconducting YBCO conductor-on-round-core (CORC) cables *Supercond. Sci. Technol.* **27** 125008
- [18] Anvar V A *et al* 2018 Bending of CORC® cables and wires: finite element parametric study and experimental validation *Supercond. Sci. Technol.* **31** 115006
- [19] De Marzi G, Celentano G, Augieri A, Muzzi L, Tomassetti G and Della Corte A 2015 Characterization of the critical current capabilities of commercial REBCO coated conductors for an HTS cable-in-conduit conductor *IEEE Trans. Appl. Supercond.* **25** 1–4
- [20] Gao P *et al* 2019 Inter-strand resistance and AC loss in resin-filler impregnated ReBCO Roebel cables *Supercond. Sci. Technol.* **32** 125002
- [21] Kovacs C, Majoros M, Sumption M D and Collings E W 2019 Magnetization measurements of CORC TM and roebel type YBCO cables for accelerators using a ±3-T dipole magnetometer *IEEE Trans. Appl. Supercond.* **29** 1–5
- [22] Uglietti D, Bykovsky N, Wesche R and Bruzzone P 2015 Development of HTS conductors for fusion magnets *IEEE Trans. Appl. Supercond.* **25** 1–6
- [23] Celentano G, Vannozzi A, De Marzi G, Marchetti M, Augieri A, Di Zenobio A, Fabbri F, Muzzi L, Rufoloni A and Della Corte A 2019 Bending behavior of HTS stacked tapes in a cable-in-conduit conductor with twisted al-slotted core *IEEE Trans. Appl. Supercond.* **29** 1–5
- [24] Sheng J, Vojenčiak M, Terzioglu R, Frolek L and Gomory F 2017 Numerical study on magnetization characteristics of superconducting conductor on round core cables *IEEE Trans. Appl. Supercond.* **27** 1–5
- [25] Otten S, Dhallé M, Gao P, Wessel W, Kario A, Kling A and Goldacker W 2015 Enhancement of the transverse stress tolerance of REBCO Roebel cables by epoxy impregnation *Supercond. Sci. Technol.* **28** 065014
- [26] Nijhuis A, Ten Kate H H J, Bruzzone P and Bottura L 1996 Parametric study on coupling loss in subsize ITER Nb/sub 3/Sn cabled specimen *IEEE Trans. Magn.* **32** 2743–6
- [27] Nijhuis A, Kate H H J, Duchateau J L and Bruzzone P 1996 Coupling Loss Time Constants in Full-Size Nb₃Sn CIC Model Conductors for Fusion Magnets *Advances in Cryogenic Engineering Materials* (Boston, MA: Springer US) pp 1281–8
- [28] Hidnert P and Krider H 1952 Thermal expansion of aluminum and some aluminum alloys *J. Res. Nat. Bur. Stand. (1934)*. **48** 209–20
- [29] Bagrets N, Goldacker W, Schlachter S I, Barth C and Weiss K-P 2014 Thermal properties of 2G coated conductor cable materials *Cryogenics (Guildf)* **61** 8–14

- [30] Sumption M, Collings E, Scanlan R, Nijhuis A, Ten Kate H H, Kim S, Wake M and Shintomi T 1999 Influence of strand surface condition on interstrand contact resistance and coupling loss in NbTi-wound Rutherford cables *Cryogenics (Guildf)* **39** 197–208
- [31] Nijhuis A and Ten Kate H H J 2000 Surface oxidation and interstrand contact resistance of Cr-coated Nb₃Sn and bare NbTi strands in CICC's *Adv. Cryog. Eng. Mater.* **46** 1083–90
- [32] Collings E W 2006 Influence of pre-heat-treatment condition on interstrand contact resistance in Nb₃Sn Rutherford cables by calorimetric AC-loss measurement. *AIP Conf. Proc.* vol 824 (AIP) pp 851–8
- [33] Nijhuis A, Ten Kate H H J, Pantsyrny V and Santini M 2000 Interstrand contact resistance and AC loss of a 48-strands Nb/sub 3/Sn CIC conductor with a Cr/Cr-oxide coating *IEEE Trans. Appl. Supercond.* **10** 1090–3
- [34] Nijhuis A, Ten Kate H H, Duchateau J-L and Decool P 2001 Control of contact resistance by strand surface coating in 36-strand NbTi CICC's *Cryogenics (Guildf)* **41** 1–7
- [35] Yagotintsev K A *et al* 2019 Overview of verification tests on AC loss, contact resistance and mechanical properties of ITER conductors with transverse loading up to 30 000 cycles *Supercond. Sci. Technol.* **32** 105015
- [36] Lu J, Goddard R, Han K and Hahn S 2017 Contact resistance between two REBCO tapes under load and load cycles *Supercond. Sci. Technol.* **30** 045005
- [37] Nijhuis A, Ilyin Y, Abbas W, Ten Haken B and Ten Kate H H J 2004 Change of interstrand contact resistance and coupling loss in various prototype ITER NbTi conductors with transverse loading in the twenty cryogenic cable press up to 40,000 cycles *Cryogenics (Guildf)* **44** 319–39
- [38] Terzioğlu R, Vojenčiak M, Sheng J, Gömöry F, Çavuş T F and Belenli İ 2017 AC loss characteristics of CORC® cable with a Cu former *Supercond. Sci. Technol.* **30** 085012
- [39] Wang Y, Zhang M, Grilli F, Zhu Z and Yuan W 2019 Study of the magnetization loss of CORC® cables using a 3D T-A formulation *Supercond. Sci. Technol.* **32** 025003
- [40] Lécresse T, Gheller J M, Louchart O, Rey J M and Tixador P 2012 Critical current and junction between pancake studies for HTS coil design *Phys. Procedia.* **36** 681–6
- [41] Wilson M 1983 *Superconducting Magnets* (Oxford: Clarendon Press) pp 335
- [42] Shen B, Coombs T and Grilli F 2019 Investigation of AC loss in HTS cross-conductor cables for electrical power transmission *IEEE Trans. Appl. Supercond.* **29** 1–5